Global and Planetary Change

The nexus among long-term changes in lake primary productivity, deep-water anoxia, and internal phosphorus loading, explored through analysis of a 15,000-year varved sediment record

--Manuscript Draft--

Manuscript Number:	GLOPLACHA-D-21-00106R1
Article Type:	Research paper
Keywords:	Internal phosphorus loadings; natural eutrophication; anoxia; Late glacial/Holocene; Paleolimnology; Switzerland
Corresponding Author:	Luyao Tu Universitat Bern Bern, Bern SWITZERLAND
First Author:	Luyao Tu
Order of Authors:	Luyao Tu
	Adrian Gilli, Dr.
	André Lotter, Prof. Dr.
	Hendrik Vogel, Dr.
	Madeleine Moyle
	John Boyle, Dr.
	Martin Grosjean, Prof.Dr.
Abstract:	Increased cultural eutrophication since the 20th century, caused by phosphorus (P) enrichment, has become a major problem worldwide. In deep, stratified lakes, eutrophication-induced hypolimnetic anoxia often stimulates the release of labile P from the sediment into the water column. This positive feedback, termed internal P loading, maintains or even accelerates eutrophication. However, most studies on internal P loading have focused on recent times. Little is known about whether such positive feedbacks caused by labile P release from sediments also played a role under natural conditions with little or no human impact. We investigated a high-resolution 15,000-year sediment record of paleoproduction, anoxia, and five sedimentary P fractions from a small, deep lake, Soppensee, on the Swiss Central Plateau. We estimated long-term qualitative internal P loading by comparing the Holocene record of diatom-inferred epilimnetic total P (DI-TP) concentrations with labile P fraction (Fe-P) concentrations in sediments under changing trophic state, redox, and lake mixing regimes. Intensified P cycling from sediments into the water column (enhanced internal P loading) apparently occurred as a positive feedback to natural eutrophication with persistent bottom-water anoxia during the early to mid-Holocene (~9000–6000 cal BP). However, this positive feedback was not inferred for other eutrophic phases. Fe-rich layers formed during seasonal mixing of the lake in the late Holocene (~2000–200 cal BP) and magnetite-type minerals produced by magnetotactic bacteria (MTB) internal P loading during anoxic phases in the mid- to late Holocene (~6000–2000 cal BP) appeared to prevent internal P loading. MTB presence resulted in high concentrations of potentially labile Fe-P in sediments. Our study demonstrates the potential contribution of internal P loading during long-term natural eutrophication of deep stratified lakes and has wide implications for lake management and restoration. Our results highlight the importance of the coupled geochemical cycles of P and Fe in the long-term trophic state evolution of stratified, ferruginous, low-sulfate-water lakes, conditions that have been reported to serve as analogs for the Archaean Ocean.
Suggested Reviewers:	Pierre Francus, Prof. Dr. INRS: Institut national de la recherche scientifique pierre.francus@ete.inrs.ca Expert in environmental sedimentology, paleolimnology, image analysis, geochemistry, Quaternary science; no joint publications or projects.
	Gertrud Nürnberg, Dr.

	gkn@fwr.ca Expert in limnology, P cycling and (internal) P loadings, eutrophication
	Olga Tammeorg, Dr. University of Helsinki olga.tammeorg@helsinki.fi Expert in limnology, anoxia of freshwater systems, regulating internal phosphorus loading and water quality in the lakes.
	Sebastian Naeher, Dr. Organic Geochemistry Laboratory (OGL), GNS Science, Christchurch, New Zealand s.naeher@gns.cri.nz Expertise: lake sediments, geochemistry, anoxia, biomarkers and pigments, hyperspectral imaging
	Michael Hupfer, Dr. Leibniz-Institute of Freshwater Ecology and Inland Fisheries, IGB Berlin hupfer@igb-berlin.de Expertise in lake internal P cycles and biogeochemical processes in sediments.
	Daniel Ariztegui, Dr. Prof., University of Geneva daniel.ariztegui@unige.ch Expert in paloelimnology, limnogeology, biogeochemical cycles in lakes
Opposed Reviewers:	
Response to Reviewers:	

The nexus among long-term changes in lake primary productivity, deep-water anoxia, and internal phosphorus loading, explored through analysis of a 15,000-year varved sediment record

Luyao Tu [a, *], Adrian Gilli [b], André F. Lotter [c], Hendrik Vogel [d], Madeleine Moyle [e], John F Boyle [e], Martin Grosjean [a]

[a] *Institute of Geography & Oeschger Centre for Climate Change Research, University of Bern, Hallerstrasse 12, 3012 Bern, Switzerland*

[b] *Geological Institute, ETH Zürich, Sonneggstrasse 5, 8092 Zürich, Switzerland*

[c] *Institute of Plant Sciences & Oeschger Centre for Climate Change Research, University of Bern, Altenbergrain 21, 3013 Bern, Switzerland*

[d] *Institute of Geological Sciences & Oeschger Centre for Climate Change Research, University of Bern, 3012, Bern, Switzerland*

[e] *Department of Geography and Planning, University of Liverpool, Liverpool L69 3BX, United Kingdom*

**Correspondence to*: Luyao Tu (*luyao.tu@giub.unibe.ch*)

Abstract

Increased cultural eutrophication since the 20th century, caused by phosphorus (P) enrichment, has become a major problem worldwide. In deep, stratified lakes, eutrophication-induced hypolimnetic anoxia often stimulates the release of labile P from the sediment into the water column. This positive feedback, termed internal P loading, maintains or even accelerates eutrophication. However, most studies on internal P loading have focused on recent times. Little is known about whether such positive feedbacks caused by labile P release from sediments also played a role under natural conditions with little or no human impact. We investigated a high-resolution 15,000-year sediment record of paleoproduction, anoxia, and

five sedimentary P fractions from a small, deep lake, Soppensee, on the Swiss Central Plateau. We estimated long-term qualitative internal P loading by comparing the Holocene record of diatom-inferred epilimnetic total P (DI-TP) concentrations with labile P fraction (Fe-P) concentrations in sediments under changing trophic state, redox, and lake mixing regimes. Intensified P cycling from sediments into the water column (enhanced internal P loading) apparently occurred as a positive feedback to natural eutrophication with persistent bottom-water anoxia during the early to mid-Holocene (~9000–6000 cal BP). However, this positive feedback was not inferred for other eutrophic phases. Fe-rich layers formed during seasonal mixing of the lake in the late Holocene (~2000–200 cal BP) and magnetite-type minerals produced by magnetotactic bacteria (MTB) internal P loading during anoxic phases in the mid- to late Holocene (~6000–2000 cal BP) appeared to prevent internal P loading. MTB presence resulted in high concentrations of potentially labile Fe-P in sediments. Our study demonstrates the potential contribution of internal P loading during long-term natural eutrophication of deep stratified lakes and has wide implications for lake management and restoration. Our results highlight the importance of the coupled geochemical cycles of P and Fe in the long-term trophic state evolution of stratified, ferruginous, low-sulfate-water lakes, conditions that have been reported to serve as analogs for the Archaean Ocean.

Key words: Internal phosphorus loadings; natural eutrophication; anoxia; Late glacial/Holocene; Paleolimnology; Switzerland

1. Introduction

Human-induced eutrophication since the 20th century, also known as cultural eutrophication, has become a major environmental threat to freshwater ecosystems worldwide. It can create toxic algae blooms and result in deep-water hypoxia or even anoxia among other adverse effects (Paerl, 1988). In most cases, lake eutrophication is attributed to excessive phosphorus (P) inputs from either external or internal loads because P is often the limiting nutrient for lake primary production (Worsfold et al., 2016). There is increasing recognition that lake internal P loading (i.e. P released from sediments into the water column) can trigger a positive feedback

of eutrophication, delaying lake recovery after reducing external P loadings (Orihel et al., 2017). This holds particularly true for seasonally stratified, deep lakes, in which hypolimnetic anoxia caused by thermal and/or eutrophication-related biochemical stratification is expected to trigger effective P recycling from surface sediments back into the water column (Lepori and Roberts, 2017; Tu et al., 2019). Hypolimnetic anoxia or meromixis-induced sediment-P release in deep eutrophic lakes has received increasing attention (Cyr et al., 2009; Nürnberg et al., 2018). In stratified eutrophic lakes, the mineralization of organic matter (OM) tends to cause depletion of dissolved oxygen in deep waters, leading to the reductive dissolution of Fe oxyhydroxides and release of adsorbed P back into bottom waters (Steinsberger et al., 2017). Studies in two seasonally stratified eutrophic lakes in Switzerland (Tu et al., 2019; 2020) have demonstrated that enhanced internal P loading and P recycling lead to a depletion of labile P in sediments.

Besides such anthropogenic drivers as residential, industrial, and agriculture discharges, natural drivers can also be responsible for lake eutrophication and hypolimnetic anoxia in deep lakes. For example, higher lake surface temperatures caused by climate warming very likely prolong the growing season for phytoplankton and thus strengthen stratification, ultimately leading to an elevated and growing risk of eutrophication and anoxia in deep lakes (Straile et al., 2003). Furthermore, temperate deep lakes in Europe have mostly been found to be naturally nutrient-rich as a consequence of their geological or geomorphological settings and ontogenesis (Kirilova et al., 2009; Makri et al., 2020; Sanchini et al. 2020).

For decades, many researchers have investigated the potential of sediment-P release using different P fractions in sediments and their potential bioavailability (Gao et al., 2005; Kapanen, 2008). Net burial of labile P fractions in sediments, in combination with productivity, redox, and lake mixing proxies, might shed light on P cycling and internal P loads as well as feedbacks in the past prior to human influence. However, most of the empirical and modeling research dealing with internal P loading has focused on timespans of a few decades (Katsev and Dittrich, 2013) and on shallow, polymictic, well-oxygenated lakes (Søndergaard et al., 2001). There

remains a lack of long-term (i.e., Holocene and longer) records of sediment-P fraction retention, eutrophication, and anoxia history, in particular in stratified, deep lakes. This has hampered efforts to reliably test whether past internal P loading and related positive feedbacks sustaining eutrophication also operated on long time scales under natural or early-anthropogenic-impact conditions.

Soppensee is an ideal site to study this question because it is a deep, eutrophic lake that possesses a sediment record with annual laminations (varves), and its sediments therefore have an exceptionally good chronology. Moreover, a record of diatom-inferred epilimnetic total P (DI-TP) concentrations is available for the entire Holocene (Lotter, 2001), which provides quantitative information about the past lake-water P concentrations.

In this study, we aimed to answer three research questions: 1) How did concentrations of different P fractions in Soppensee sediments and internal P loading of the lake vary during the periods before human disturbance? 2) What was the relationship through time between concentrations of labile P forms in sediments and both diatom-inferred water-column TP (DI-TP) concentrations and pigment-inferred lake primary production? 3) Did eutrophication-driven hypolimnetic anoxia promote internal P loading, as reflected by concurrent low concentrations of labile P fractions in sediments and elevated DI-TP values? To answer these questions, we combined a Holocene high-resolution paleoproduction and anoxia record with a record of five sediment P fractions and DI-TP concentration data. If DI-TP is assumed to be an unbiased estimate of the epilimnetic total P, then this approach enables us to investigate the relationship between epilimnetic total P concentrations and sedimentary labile P fraction concentrations under changing primary production and lake mixing regimes throughout the Holocene. We hypothesize that differences between the DI-TP and sediment labile P records enable qualitative inferences of internal P loading that indicate a positive feedback of natural eutrophication.

2. Study site

Soppensee is a small, hard-water lake situated on the Swiss Central Plateau at 596 m above sea level (47°05'30"N, 08°05'E). This kettle-hole lake was formed after the retreat of the Reuss glacier at the end of the last glaciation (Lotter, 1989). It has a small surface area (0.227 km^2) relative to its maximum water depth (Z_{max} =27 m; the relative depth = ~5%). The lake does not have surface inflows and is mainly fed by groundwater and seasonal surface run-off with negligible detrital inputs from a small calcareous sandstone catchment of 1.6 km^2. The outflow leaves the lake in the northwest (Fig. 1b). The water volume amounts to 2.9×10^6 m^3 with a residence time of ~ 3.1 years (Fischer, 1996).

Soppensee sediments are characterized by well-preserved varves that provide a continuous record of most of the Early-Mid Holocene and part of the Late glacial (Lotter 1989). The sediments are very well dated with varve counting paired with ^{14}C dates (Hajdas and Michczyński, 2010) and provide an excellent archive for chironomids (Hofmann, 2001), pollen (Lotter, 1999), and diatoms (Lotter, 2001). According to the DI-TP concentrations record, Soppensee remained meso- to eutrophic throughout the Holocene (Lotter, 2001). Today, the lake is classified as eutrophic to hypertrophic with lake-water total P concentrations in the range of 50–116 µg L^{-1} (Müller et al., 1998). Currently, Soppensee is holomictic with strong thermal and chemical stratification and hypolimnetic anoxia in summer (Gruber et al., 2000). Mixing mostly occurs in fall and winter.

The catchment area of Soppensee is farmed intensively, with arable and pastoral uses accounting for 82% of the catchment area and wooded areas representing 12% (Langenegger et al., 2019). The wooded areas are composed of mixed forest dominated by *Picea abies* (spruce; planted) and *Fagus sylvatica* (beech). A temperate and oceanic climate prevails in the region, with July (~17.6 °C) the warmest month and January (~ -0.3 °C) the coldest.

3. Materials and methods

3.1. Sediment sampling and chronology

In August 2008, several UWITEC piston cores with overlapping sequences were retrieved from the deepest part of the lake at a water depth of 27 m (47°05'26.6"N, 08°04'49.4"E; Fig. 1a, b). After core collection, the cores were tightly sealed and stored in a cold room at 4°C before opening. In 2019, the cores were split lengthwise in two halves, A and B, and the oxidized surfaces were described according to Schnurrenberger et al. (2003). The A-half cores were used for visual correlation and non-destructive scanning techniques including x-ray fluorescence (XRF) and hyperspectral imaging (HSI). The B-half cores were subsampled for destructive geochemical analysis such as pigment analysis and P extraction. The composite core So08-3 examined in this study was assembled from three overlapping cores based on stratigraphic marker layers and XRF data correlation. The composite sequence has a total length of 571 cm, covering the past ~15,000 years (Fig. 1c). The chronology of core So08-3 is based on the correlation of XRF data and sedimentary marker layers to core So08-01/2 dated by Hajdas and Michczyński (2010) and van Raden (2012) using 42 tie points (see Table S1 and Fig. S1 in supplementary material).

3.2. Sediment lithology

Previous research (Hajdas and Michczyński, 2010; Kind et al., 2012; Gierga et al., 2016) has shown that the uppermost ~6 m sediments of Soppensee are organic-rich lacustrine deposits that are divided into six sedimentary units (A to F) based on lithological characteristics.

Unit A (571–548 cm in Core So08-3; Fig. 1c) contains detrital deposits with light-grey silty clays deposited between ~15,115 and 13,800 cal BP during the deglaciation of the Swiss Plateau (see Gierga et al. 2016). In unit B (548–474 cm), sediments are dark-brownish and rich in organic matter and carbonates. As Fischer (1996) described, unit B is partly laminated with Fe-rich layers formed in the Late-glacial period. According to Gierga et al. (2016), unit B can be attributed to the Allerød interstadial (~13,800–12,700 cal BP) and the Younger Dryas (YD, ~12,700–11,500 cal BP). The Laacher See tephra (LST), dated to ~12,800 cal BP (Hajdas and Michczyński, 2010), is found within this unit prior to the onset of the YD. Unit C (474–350 cm) consists of continuous biogenic calcite varves formed during the early to mid-

Holocene until ~6000 cal BP. In unit D (350–187 cm; ~6000–2000 cal BP), sediments are rich in organic matter with an overall very dark color. Vivid blue crystals (vivianite) are visible at some spots from parts of the oxidized core surface in unit D. Unit E (187–35 cm) represents the period ~2000–200 cal BP and consists of very faint laminations and organic-rich sediments with lighter color than unit D. The uppermost unit, F, (above 35 cm) consists of light brown sediments deposited during the last ~200 years.

3.3. Geochemical methods

The semi-quantitative elemental composition was measured on the fresh sediment surface of core So08-3 using an ITRAX XRF Core Scanner (Cox Ltd.) equipped with a Cr-Anode-Tube set to 30 kV and 50 mA at the Institute of Geological Sciences, University of Bern. Measurements were made at 5-mm contiguous intervals using an integration time of 30 s. Prior to scanning, the sediment surface was carefully cleaned and smoothed. All XRF data are given as total counts per area (cts). For the interpretation of selected XRF elements, Ti was used as an indicator of lithogenic content; Ca of endogenic calcite content; and Mn of water column redox conditions (van Raden, 2012).

The HSI scans were made with a Specim Ltd. single core scanner equipped with a hyperspectral linescan camera (Specim PFD-CL-65-V10E) in the visual to near-infrared range (VNIR, 400–1000 nm) following the methodology in Butz et al. (2015). Parameters were set to a spatial resolution of ~75 µm per pixel and a spectral sampling of 1.57 nm (binning of 2). Relative absorption band depth (RABD) indices were calculated to quantify the absorbance troughs caused by sedimentary chloropigments and bacteriopheophytins. The $RABD_{567\text{-}769}$ spectral index was retrieved from a local minimum of the absorption feature between wavelengths of 567 nm and 769 nm after the method in Schneider et al. (2018), as described in Fig. S2 of supplementary material. The $RABD_{567\text{-}769}$ spectral index indicates total chlorophylls and diagenetic products in sediments, from which lake primary production can be inferred (Schneider et al., 2018; Makri et al., 2020). The $RABD_{845}$ spectral index represents bacteriopheophytins *a* and *b*, a specific biomarker diagnostic for purple sulfur bacteria (PSB).

PSB are anoxygenic phototrophic bacteria that live at the chemoclines of stratified lakes with oxic–anoxic interfaces; thus the presence of PSB indicates seasonal hypolimnetic anoxia or meromixis in the lake with light penetration to the chemocline (Butz et al., 2016; Zander et al., 2021).

The pigment extraction of 32 sediment samples (1 cm slices) followed the method in Amann et al. (2014), which was applied to ~ 0.1–0.5 g freeze-dried homogenized sediments using 100% acetone (HPLC grade) solution. Pigment concentrations in extracts were determined with a Shimadzu UV-1800 spectrometer. We used the molar extinction coefficients for chlorophyll-*a* and chlorophyll-*a* derivatives (here green pigments) from Jeffrey and Humphrey (1975) and for bacteriopheophytin-*a* (Bphe-*a*) from Fiedor et al. (2002). $RABD_{567\text{-}769}$ and $RABD_{845}$ values were calibrated to spectrophotometrically determined concentrations (µg g^{-1} dry sediments) of green pigments and Bphe-*a*, respectively, using linear regression models following Butz et al. (2015). The calibration models were validated by R^2 and the root mean squared errors of prediction (RMSEP) (Fig. S3). Residual analyses of the linear calibration models (Fig. S4 and S5) revealed that three samples cause a slight tailing in the normal QQ-plot (Fig. S4b and S5b) and higher leverage (Fig. S4d and S5d); a weak heteroscedastic pattern is visible in Fig. S4c and S5c. However, the Shapiro-Wilk and the Kolmogorov-Smirnov tests both indicate most likely normal distributions of the residuals for the two linear regression models; thus, the inferences from the two calibration models are valid.

The sediment P fractionation procedure in this study principally followed the harmonized protocol developed by the standards, measurements and testing (SMT) of the European Commission as modified in Ruban et al. (1999) and Ruban et al. (2001) based on Williams et al. (1976). The SMT protocol consists of three independent extraction procedures and defines five P fractions: non-apatite inorganic P (P bound to Fe, Al and Mn oxides and hydroxides, hereafter referred to as Fe-P), apatite P (calcium bound P, hereafter Ca-P), inorganic P, organic P, and total P. Fe-P in sediments is a labile P source under anoxic conditions and in high pH environments (Rydin, 2000), which can be considered potentially bioavailable and

may be released from the sediments into the water column, contributing to internal P loading in lakes (Zhu et al., 2013). Fe-P includes the redox-sensitive Fe bound P (NaBD-P) in Tu et al., (2019) and is considered as the labile P form in this study. Inorganic P includes Fe-P, Ca-P, and other inorganic P species in sediments. Ca-P in sediments is considered relatively stable and non-bioavailable, and organic P partly bioavailable. In this study, we focus on Fe-P, Ca-P, and organic P. We made slight modifications to the SMT protocol: a) In each extraction step, we used 40 mL (instead of 20 mL) extractant (i.e., NaOH and HCl) for ~0.2 g aliquots of freeze-dried homogenized sediments. The lower dry sediment weight-to-extractant volume ratio (1:200) was to avoid the saturation limit of P released from the solid phase. b) Two 1 M NaCl rinse steps (20 mL) were added after each main extraction step. The P determined in rinsing solutions was added to the corresponding P pools to maximize the extraction efficiency. Following each extraction and rinsing step, supernatant was collected after centrifugation at 4000 rpm for 15 min at room temperature.

Phosphate concentrations in all unfiltered extracts were determined spectrophotometrically with the malachite green method (Ohno and Zibilske, 1991) and the absorbance measured at 610 nm (Shimadzu UV-1800 spectrophotometer). The details of the colorimetrical analyses can be found in Tu et al. (2019). Certified reference sediment material (CRM) BCR-684 was used for quality control of the analytical data and efficiency of the extraction procedure. The analytical results for BCR-684 are in good agreement with the certified contents from the certification report for the SMT procedure (Table S2).

3.4. Data analysis

Statistical analyses were performed using R 3.4.2 (R Core Team, 2017). The packages ‘ggplot2’ (Wickham, 2016) and ‘corrplot’ (Wei and Simko, 2017) were used for data analyses and visualization. Pigment concentrations data were aggregated averagely to the time resolution of P data prior to statistical analyses. Some variables are non-normal distributed (using the Shapiro-Wilks test; Royston, 1995). To investigate the relationships between

variables, Spearman's correlation analysis was performed on the centered and standardized dataset.

4. Results and interpretation

4.1. Time series of geochemical data

Fig. 2 shows that HSI-pigment, P fractions, and XRF data exhibit distinctive features across the six stratigraphic units (A to F in Fig. 1c). The long-term phase relationship between Fe-P data and lake paleoproduction history reveals an approximately coherent pattern across the units. This coherence is confirmed by a significantly positive correlation between Fe-P and green pigments (Spearman's correlation coefficient (ρ) = 0.5, p-value < 0.05; Fig. S6b). Labile P (Fe-P) is the dominant P fraction in most periods (averagely constitutes 54% of the sum of the three P fractions; Fig. S8b). The labile P fraction exhibits a pattern very similar to total P and inorganic P over time (Fig. 2). The Fe- and Mn-rich laminae (Fischer, 1996) and calcite varves (Hajdas and Michczyński, 2010) coincide with relatively high XRF Fe and Mn counts and high Ca counts, respectively (Fig. 2). Fig. 3 shows four distinct 2-cm example sections with corresponding high-resolution HSI-pigment data from the Late-glacial (Fig. 3a and b) and Holocene periods (Fig. 3c and d). Fig. 4 primarily compares sedimentary Fe-P data with the DI-TP concentration record (Lotter, 2001) and with centennial-scale records of lake paleoproduction and anoxia. DI-TP data are not available for the Late-glacial period (units A and B) because of diatom dissolution in these sediments. Instead, we compared HSI-pigment-inferred lake primary production with the Fe-P stratigraphy (Fig. 4d and f).

In unit A, the deglaciation period (~15,115–13,800 cal BP; Gierga et al., 2016), green pigments and Bphe-*a* values remain at minimal levels, indicative of low lake primary production with a poorly stratified water column. High Mn counts (Fig. 2) imply a well-mixed water column; high Ti counts (Fig. S9) imply high quantities of lithogenic sediments. The values for the Fe-P and all the other P fractions are very low.

In unit B (~13,800–11,500 cal BP), green pigments and Bphe-*a* values generally increase, as do concentrations of Fe-P in sediments. The very beginning of unit B (~13,800–13,600 cal BP, latest part of the Allerød interstadial; Gierga et al. 2016) exhibits the first distinct peaks of green pigments and Bphe-*a* concentrations. This suggests substantially enhanced lake primary production and strongly stratified and anoxic conditions; Bphe-*a* values are well above the limit of quantification (9.7 µg g^{-1} dry sediments) for more than 40 years, which in turn suggests strongly stratified and mostly anoxic, maybe even meromictic conditions (Fig. 3a). Concurrently, Fe-P concentrations in sediments remain low during the peak of the green pigments and Bphe-*a*. During the remainder of the Allerød interstadial (~13,600–12,700 cal BP), lake primary production is still relatively high; Bphe-*a* concentrations drop to substantially lower levels, yet counts of Fe and Mn are high, which suggests seasonally oxygenated bottom waters. In the same period, Fe-P and total P concentrations in sediments increase sharply but then decrease to low values at the transition to the YD cold phase at ~12,700 cal BP. During the YD, Bphe-*a* is largely absent or close to the detection limit for several years (Fig. 3b), indicating consistently good oxygenation of the hypolimnion. This is also confirmed by high Mn counts (Fig. 2). Lake paleoproduction in this phase was relatively low, except for a small peak at ~12,400 cal BP. Concurrently, low values of the Fe-P are found throughout this period.

Unit C is characterized by relatively high Bphe-*a* and aquatic production, as well as overall increased values of all P fractions in the sediments (Fig. 2). At the onset of the early Holocene (~11,500–11,000 cal BP), green pigments and Bphe-*a* increase rapidly to a relative maximum between ~11,200 and ~11,000 cal BP, whereas the Fe-P value is still low. Subsequently (11,000–9000 cal BP), lake primary production decreases slightly, yet Fe-P values increase slightly. In the early Holocene (11,500–9000 cal BP), Bphe-*a* values are clearly higher, with multiple local peaks, indicating a strongly stratified water column and sustained anoxia in the hypolimnion for most of this period. This interpretation is supported by constantly declining Mn counts in this phase (Fig. 2), suggesting less frequent mixing of the bottom water. Slightly low but increasing DI-TP concentrations from ~11,500 cal BP to 9000 cal BP coincide with

289 moderately low values of Fe-P (Fig. 4c and d). The following early to mid-Holocene (~9000–
290 6000 cal BP) is characterized by relatively high and increasing lake primary production and
291 constantly elevated Bphe-*a* concentrations. The example section from this period (Fig. 3c)
292 shows high concentrations of Bphe-*a* above the detection limit for several years, which is
293 indicative of a strongly stratified water column under mostly meromictic conditions. The
294 persistent anoxia in the bottom water is further supported by very low Mn counts in this period
295 (Fig. 2). In contrast to a trend of increasing lake paleoproduction (Fig. 4f) and higher DI-TP
296 concentrations (Fig. 4c), Fe-P values decline substantially and remain at minimal levels
297 between ~9000 and 6000 cal BP (Fig. 4d).

298 In unit D, from the mid- to late-Holocene (~6000–2000 cal BP), aquatic production further
299 increases and remains high (Fig. 2). High Bphe-*a* well above the detection limit occurs
300 throughout most of this unit (Fig. 2), which indicates strongly stratified conditions with anoxia.
301 This interpretation is confirmed by constantly low Mn counts in this period. Both DI-TP and,
302 interestingly, Fe-P records exhibit considerably increased and more variable values (Fig. 4b
303 and c).

304 In unit E, from ~2000 to 200 cal BP, lake paleoproduction declines slowly, and Bphe-a remains
305 at very low concentrations overall (Fig. 2). The example section from this period (Fig. 3d)
306 displays that Bphe-*a* concentrations are close to the detection limit (~9.7 µg g^{-1} dry sediments)
307 for several years. This indicates the absence of a stable chemocline. The Fe- and Mn-rich
308 laminae present in this phase (Fig. 2) most likely imply seasonal mixing of the water column
309 with strong anoxia during the summer season. Lower DI-TP concentrations are synchronous
310 with relatively high but continuously decreasing Fe-P values (Fig. 4c and d).

311 In the most recent 200 years (unit F), lake primary production increased considerably; Bphe-
312 *a* concentrations stay at sustained minimal levels (Fig. 2), indicating the general absence of a
313 persistent chemocline. However, Mn counts are very low in this period (Fig. 2), which still
314 suggests seasonal hypolimnetic anoxia. DI-TP concentrations reach the highest levels,
315 whereas sedimentary Fe-P concentrations decrease to very low values.

4.2 Centennial-scale relationship between lake primary production and sediment labile P

Over the past ~15,000 years and superposed on the long-term (multi)millennial trends, at the shorter-term (centennial) time scale, there is an inverse relationship between sediment Fe-P concentrations and both lake primary production and anoxia (Fig. 4d-f). In many but not all cases, relative minima (maxima) in lake paleoproduction and anoxia tend to correspond to relative maxima (minima) of Fe-P (dashed blue and red lines in Fig. 4; Fig. S10c-e). For example, during the Late-glacial period represented by unit B, enhanced lake primary production with stronger anoxia at ~13,700 cal BP and ~12,400 cal BP coincides with relatively low values of Fe-P (see dashed red lines). In contrast, lake primary production and anoxia indicators display decreased values at ~13,500 cal BP and 13,000 cal BP, which corresponds to local peaks of Fe-P (see dashed blue lines). Similar observations can be made in other units during most of the Holocene, pointing to a negative relationship between sedimentary Fe-P and both paleoproduction and anoxia at short (multidecadal to centennial) time scales.

5. Discussion

5.1. Late-glacial and Holocene lake trophic state evolution and anoxia history

Here we present a Late-glacial and Holocene overview of aquatic production and anoxia in Soppensee reconstructed from HSI-inferred sedimentary pigments data. Diatom assemblages and pigment concentrations are two palaeolimnological indicators commonly used to infer past changes in lake trophic status (Davidson and Jeppesen, 2013). In Soppensee, DI-TP concentrations (Lotter, 2001) displayed mesotrophic to eutrophic conditions during most of the Holocene, suggesting that Soppensee is a naturally nutrient-rich lake. Our pigment-based lake primary production record generally exhibits a pattern coherent with the DI-TP record throughout the Holocene (Fig. 4c and f). For example, both records show moderately high levels from 11,500 to 9,000 cal BP, very high levels from 6000 to 2000 cal BP, and decreased

values from ~2000 to 200 cal BP. This coherence confirms that HSI-inferred green pigment data reliably capture epilimnetic aquatic production in Soppensee.

The green pigments record (Fig. 2) suggests that the lake primary production was relatively low before ~13,800 cal BP and in the YD cold phase (~12,700–11,500 cal BP), but increased as a consequence of increasing nutrient enrichment during the Allerød interstadial (~13,800–12,700 cal BP) and for most of the Holocene. From ~8000 to ~3000 cal BP, early human impact was very limited and there is no evidence for strong human disturbance or extensive forest clearance in the catchment (Lotter, 1999; 2001); thus, the long-term eutrophication that Soppensee underwent during that time was mostly natural. Lake primary production in Soppensee is slightly positively correlated with chironomid-inferred summer temperature from the Alpine region (Heiri, et al., 2015; Spearman's correlation coefficient (ρ) = 0.22, p-value < 0.05, Fig. S7). The lake became more eutrophic (higher primary production and higher DI-TP) during warm climatic conditions in the Allerød interstadial and in the mid-Holocene after ~6000 cal BP. During the Allerød interstadial, summer temperature increased in Central Europe (Fig. 4a), and in the mid-Holocene, warm and humid climate conditions prevailed on the Swiss Plateau (Rey et al., 2020). These climate factors likely prolonged the growing season of lake phytoplankton and leached more nutrients from developing catchment soils into the lake, which then promoted natural eutrophication in Soppensee during these long warm phases. Between ~3000 and 200 cal BP, and especially from ~2000 to 200 cal BP, strong human impact with intense land use occurred in the Soppensee catchment (Lotter, 1999), but less eutrophic conditions prevailed in Soppensee (Fig. 4e). Decreased aquatic production during the late Holocene was also reported from Lake Łazduny and Lake Żabińskie in Poland (Sanchini et al., 2020; Zander et al., 2021). Late Holocene climate cooling, particularly in summer (Davis et al., 2003; Fig. 4a, Heiri, et al., 2015), can partly explain this phenomenon. Since the 20th century, lake primary production has increased sharply as a result of cultural eutrophication (see green pigments record; Fig. 2). We attribute this observation to anthropogenic nutrient inputs from the catchment into the lake.

Under pre-anthropogenic conditions (mainly before ~3000 cal BP), strong stratification and anoxic conditions in the hypolimnion (high Bphe-*a*; Fig. 2) tended to occur during times of higher lake primary production (high green pigments) and warmer summers (Fig. 4a), for instance ~13, 800–13,600 cal BP and ~8000–4000 cal BP. This interpretation is confirmed by significantly positive correlations between lake anoxia (Bphe-*a*) and both lake primary production (green pigments) and summer temperature (ρ = 0.51 and 0.75, respectively, p-value < 0.05, Fig. S7). Similar results (higher lake production and higher summer temperatures causing stronger stratification and anoxia) have also been found in other small lakes in Europe, for example, Moossee in Switzerland (Makri et al., 2020) and Lake Jaczno (Makri et al., 2021) and Lake Żabińskie (Zander et al., 2021) in Poland. However, in all these examples closed forest cover around the small lakes was also found to be an important factor favoring prolonged seasonal stratification and stable hypolimnetic anoxia (Makri et al., 2020; Zander et al., 2021). This was also the case around Soppensee during the early to mid-Holocene (~9000–3000 cal BP), when the lake catchment was covered with dense closed forest (arboreal pollen AP > 90 %; Fig. 4b; Lotter, 1999) that provided protection from the wind and promoted stable stratification and anoxia. From ~2000 cal BP until recent centuries, weaker stratification with periods of oxygen mixing into the hypolimnion is suggested by constantly low Bphe-*a* concentrations (close to the detection limit; Fig. 3d) and Fe-and Mn-rich laminae (Fig. 2). Indeed, after ~2000 cal BP, better lake mixing can be seen and was likely a result of intense forest clearance during Roman times and the Middle Ages (mostly AP < 80 %; Fig. 4a; Lotter, 2001), which increased wind-induced mixing of the water column. A similar process has been well studied in several small deep lakes of Europe, e.g. Makri et al. (2020), Sanchini et al. (2020), and Zander et al. (2021). During recent times, Mn counts in sediments of Soppensee are very low (Fig. 2), suggesting hypolimnetic anoxia. This confirms Gruber et al.'s (2000) finding that in recent times Soppensee has been holomictic but has strong chemical stratification and persistent anoxia in deep waters. However, Bphe-*a* values are very low at this time, which is likely explained by poor light conditions at the chemocline because of high

algal productivity in the photic zone. Similar observations were made in Moossee (Makri et al., 2020; Switzerland) and Lake Żabińskie (Zander et al., 2021; Poland).

5.2. Estimating internal P loading in response to lake trophic state change evolution

Labile Fe-P was the primary sedimentary P form for most of the Late glacial and Holocene (Fig. S8b). In principle, this suggests there was a high potential of sediment-P release back to the water column in Soppensee's history. Tu et al.'s (2019) conceptual model implies that deep and eutrophic lakes tend to undergo bottom-water anoxia that increases internal recycling of sedimentary labile P forms (mainly Fe-P fraction), referred to as internal P loading, a positive feedback that sustains or even accelerates epilimnetic eutrophication. As a result, the labile P fraction in sediments is depleted because it is recycled back into the water column. We investigated the possibility of such positive feedback during long-term phases of natural eutrophication to evaluate whether Tu et al.'s (2019) conceptual model is valid for Soppensee's long-term Holocene record. For these purposes, long-term qualitative internal P loading in Soppensee was inferred by comparing the record of DI-TP concentrations, a proxy for lake primary production, with sediment Fe-P data (Fig. 4c, d and f). We hypothesize that higher DI-TP but depleted sediment Fe-P demonstrates that internal P loading operated as a positive feedback to sustain eutrophication. Fig. 5 outlines four distinct phases in a conceptual model that summarizes Fe-P retention in sediments and internal P loading in response to biogeochemical P cycling coupled with Fe, primary production, and anoxia since the early Holocene.

We infer that largely high internal P loading served as a positive feedback arising from high lake primary production and deep-water anoxia from the early to mid-Holocene (~9000–6000 cal BP; Phase a in Fig. 5). That was a long period during which high DI-TP concentrations were associated with notably low values of Fe-P (Fig. 4c and d; Fig. S11). This pattern suggests mobilization of large amounts of labile Fe-P from the sediment (internal P loading) to sustain aquatic production in the photic zone. In Phase a (~9000–6000 cal BP; Fig. 5a), the lake had strongly stratified and anoxic conditions, as indicated by persistently high Bphe-*a*

(Fig. 4e). Bottom-water anoxia during times of eutrophication is expected to cause large release of Fe bound P from sediments into surface waters (Burley et al., 2001; Tu et al., 2019) and thus depleted Fe-P in sediments (Fig. 5a). This interpretation supports Tu et al.'s (2019) conceptual model.

During the mid- to late Holocene period (~6000–2000 cal BP, Phase b Fig 5), both DI-TP levels and sedimentary Fe-P values are very high (Fig. 4c and d; Fig. S11), in contrast to Tu et al.'s (2019) model. Generally, we interpret this period as one of limited sediment-P release into surface waters; thus, internal P loading might not have operated as the positive feedback of eutrophication (see Phase b in Fig. 5), although Soppensee was strongly stratified and anoxic (Fig. 4e). Ferromagnetic minerals (e.g., magnetite and hematite, magnetofossils) produced by magnetotactic bacteria (MTB) were found in Soppensee sediments deposited at that time (Kind et al., 2012), which explains the high burial rates and high amounts of sedimentary Fe-P at this time (Fig. S12 and Fig. 2): Rivas-Lamelo et al. (2017) highlighted the role of MTBs in the sequestration of P in meromictic, ferruginous low-sulfate Lake Pavin. MTB live around the chemocline, and colonization in the water column is favored by persistent stratification and high epilimnetic P concentrations (Paasche et al., 2004). Such conditions persisted in Soppensee from ~6000 to 2000 cal BP as shown by high DI-TP and high Bphe levels, and MTB were shown to be preserved in the sediments of that time as pure or oxidized magnetite minerals (Kind et al., 2012). Paasche and Larsen (2010) and Rivas-Lamelo et al. (2017) revealed that Fe oxyhydroxides produced by MTBs can escape from sulfidization and progressive reductive dissolution and, ultimately, efficiently sequester P in reduced sediments. This mechanism, in the long term, reduced internal P loading by lowering P release from sedimentary Fe-P (Phase b in Fig. 5), which is different from what occurred in Phase a (Fig. 5). As a result, very high amounts of Fe-P were preserved in the sediments during Phase b. However, throughout that time, the short-term (centennial-scale; dashed red and blue lines in Fig. 4d and f) inverse relationship between lake paleoproduction and sediment Fe-P records still generally held true. Apparently, the positive feedback between paleoproduction, anoxia,

and internal P loading that sustained eutrophic conditions still played a subordinate role on shorter time scales, but the long-term Fe-P trends in the sediment were largely controlled by MTB between 6000–2000 cal BP. Thus, Tu et al.'s (2019) model needs to be expanded and modified to account for the presence of MTB (Phase b; Fig. 5). This has implications for internal P loading and serves to explain suppressed recycling and highly efficient sequestration of Fe and P and the (early diagenetic) formation of siderite and vivianite in deep stratified ferruginous low-sulfate lakes. These lakes have recently been reported as analogs of the ferruginous euxinic Archaean ocean (Vuillemin et al., 2020; Boyko et al., 2021) where P trapping was efficient (Blake et al., 2010) and P recycling from the sediment was apparently weak (Hao et al., 2020).

The phase of the late Holocene (~2000–200 cal BP; Phase c in Fig. 5) is notable for generally decreased DI-TP concentrations, but relatively high Fe-P values (Fig. 4c and d; Fig. S11), suggesting reduced internal P loading. Sediments of this phase are marked by the occurrence of Fe- and Mn-rich laminae (Fig. 2; Fischer, 1996). The pale-brown Fe- and Mn-rich laminae are commonly formed in holomictic temperate lakes with seasonal anoxia (Zolitschka et al., 2015), in which bottom waters are seasonally oxygenated during periods of circulation (van Raden, 2012). This notion agrees well with the better mixed and less stratified water column in Soppensee at this time (Section 5.1). Previous research demonstrated that Fe-oxide layers can reduce internal P loading by hindering P release from anoxic surface sediments and favor permanent P trapping and sequestration in sediments (Zarczynski et al., 2019). Such a process very likely led to lower internal P loading between ~2000 and 200 cal BP, resulting in high amounts of Fe-P preserved in sediments (Phase c in Fig. 5). In addition, the inverse relationship between lake primary production and sediment Fe-P on centennial time scales is not clearly observable between ~2000 and 200 cal BP (Fig. 4c and e). Therefore, on both long- and short-time scales, internal P loading may not have operated as a positive feedback of eutrophication during this phase.

In the most recent 200 years (Phase d in Fig. 5), we infer high internal P loading to be the positive feedback that has sustained cultural eutrophication in Soppensee, which can be seen from high P concentrations in the water column (Fig. 4c), less frequent oxygenation of the hypolimnion (indicated by very low Mn counts; Fig. 2), and depleted Fe-P in sediments (Fig. 4d). The high internal P loading in Phase d supports Tu et al.'s (2019) conceptual model.

Because of a lack of preserved diatoms, DI-TP values are not available for the Late-glacial period (Allerød and YD). However, the frequent inverse correlation between both paleoproduction and anoxia with Fe-P during the Allerød and the beginning of the YD (Fig. 4c-e) suggests that a mechanism of strong internal P cycling, depleted Fe-P in sediments, and sustained primary production (with related anoxia) also operated in the Allerød interstadial. By contrast, for most of the YD cold phase, better oxygenation of bottom waters, together with low aquatic production and Fe-P (Fig. 4d-f), indicates low amounts of internal P cycling into surface waters to promote aquatic production. After the transition from the YD to the Holocene (~11,500–9000 cal BP), DI-TP concentrations were comparatively low while Fe-P values were moderately low, but increased slightly compared with the YD (Fig. 4c and d). This period is characterized by Fe- and Mn-enriched layers in sediments (Fig. 2; Fischer, 1996), suggesting a seasonal mixing of the water column and very likely lower internal P loading in the long term, a pattern similar to Phase c (~2000–200 cal BP; Fig. 5) discussed above. Nonetheless, Fe-P values in this period were lower than in Phase c (Fig. 4d), which may have resulted from greater release of sediment Fe-P in response to the strongly stratified water column during most of the period from 11,500 to 9000 cal BP (higher Bphe-*a* values; Fig. 4d). Between ~11,500 and 9000 cal BP, on centennial time scales, the inverse relationship between both paleoproduction and anoxia and Fe-P (Fig. 4d-f) demonstrates that internal P loading operated as a positive feedback.

We note that our core was taken from the deepest part of the lake, where the sediment P records might not reflect P dynamics, i.e., burial rates and releases, throughout the entire lake. Spatial variability and geochemical focusing (Schaller and Wehrli, 1996) in the sediment P

concentrations and forms must be considered. Because of vertical variations of the redox front and horizontal mixing, P sedimentation, net burial rates, and cycling are likely quite different between shallower and deeper parts of the lake. Sediments from shallower parts of the lake tend to be exposed to higher oxygen concentrations than those in the deepest parts (at least seasonally; Schaller and Wehrli, 1996), potentially causing better P trapping and less sediment P release into the photic zone. It is possible that in Soppensee, internal P loading inferred from the core at the deepest part of the lake is overestimated and could have been balanced to some extent by higher net burials in the shallower parts of the lake. Thus, if P release from sediments had been highly localized, in only the deepest part of the lake, it would not have substantially influenced P levels in the epilimnion, where planktonic diatoms live. Therefore, inferences for internal P loading derived from P in sediment cores from the deepest parts of the lake should be interpreted with caution; they might not reflect lake-wide P processes. Further work on spatial distribution patterns (geochemical focusing) of sedimentary P fractions from short cores across a water-depth gradient may provide important insights into whole-lake P dynamics and mass-balance modeling in deep lakes.

6. Conclusions

We propose that internal P loading has played an important role in the long-term natural eutrophication of stratified deep lakes such as Soppensee during the Late-glacial and Holocene. High internal P loading as a positive feedback of eutrophication and related anoxia were inferred in Soppensee from the early to mid-Holocene (~9000–6000 cal BP) under natural conditions and during the most recent 200 years of cultural eutrophication. However, strong recycling and depletion of labile P fractions in the sediment was not observed in other long phases of high aquatic production and anoxia. Fe-rich minerals (magnetofossils) produced by magnetotactic bacteria (MTB) and Fe-rich laminae preserved in anoxic sediments may have reduced internal P loading despite high lake primary production and anoxia between 6000 and 200 cal BP. Our study implies that the presence of (bacterially-mediated) endogenous Fe minerals that restrict P recycling and bioavailability should be

considered in conceptual models of biogeochemical P cycling on long-term (multi)millennial timescales in deep stratified eutrophic lakes. Presence of MTBs may promote P removal from the water and reduce internal P loading in lakes, which has implications for present-day eutrophication management. In future studies, it will be important to explore further other microbially mediated processes that contribute to the P cycle in similar environments.

Data availability

The data will be available at Mendeley Data Repository.

Declaration of competing interest

None.

Acknowledgements

This project was funded by the Swiss National Science Foundation (grant no. 200021-172586), a Fellowship Grant from the Chinese Scholarship Counsel, and the International PhD Fellowship from the University of Bern. Core retrieval was covered by an ETH research grant – CHIRP1 (CH1-02-08-2) and help in the field from U. van Raden, A. Birkholz, S. Jaccard and R. Hofmann is kindly acknowledged. We thank Paul Zander for help in preparing the sediment cores, hyperspectral imaging scanning, and XRF scanning. Thanks also go to Giulia Wienhues for help in preparing the sediment cores. We acknowledge Dr. Daniela Fischer and Patrick Neuhaus for their assistance in the lab. Special thanks go to Dr. Simon Milligan for English language editing. We thank Dr. Mark Brenner and an anonymous reviewer for their constructive and thoughtful comments.

Appendix A. Supplementary data

Supplementary data to this article can be found online.

Reference

552 Amann, B., Lobsiger, S., Fischer, D., Tylmann, W., Bonk, A., Filipiak, J., Grosjean, M., 2014.
553 Spring temperature variability and eutrophication history inferred from sedimentary pigments
554 in the varved sediments of Lake Żabińskie, north-eastern Poland, AD 1907–2008. Glob. Planet.
555 Change 123, 86–96. https://doi.org/10.1016/j.gloplacha.2014.10.008

556 Blake, R.E., Chang, S.J., Lepland, A., 2010. Phosphate oxygen isotopic evidence for a
557 temperate and biologically active Archaean ocean. Nature 464, 1029–1032.
558 https://doi.org/10.1038/nature08952

559 Boyko, V., Avetisyan, K., Findlay, A., Guo, Q., Yang, X., Pellerin, A., Kamyshny Jr, A., 2021.
560 Biogeochemical cycling of sulfur, manganese and iron in ferruginous limnic analog of Archean
561 ocean. Geochim. Cosmochim. Acta 296, 56–74. https://doi.org/10.1016/j.gca.2020.12.020

562 Burley, K.L., Prepas, E.E., Chambers, P.A., 2001. Phosphorus release from sediments in
563 hardwater eutrophic lakes: the effects of redox-sensitive and-insensitive chemical treatments.
564 Freshw. Biol. 46, 1061–1074. https://doi.org/10.1046/j.1365-2427.2001.00789.x

565 Butz, C., Grosjean, M., Fischer, D., Wunderle, S., Tylmann, W., Rein, B., 2015. Hyperspectral
566 imaging spectroscopy: a promising method for the biogeochemical analysis of lake sediments.
567 Appl. Remote Sens. 9, 096031. https://doi.org/10.1007/s10933-017-9955-1

568 Butz, C., Grosjean, M., Poraj-Górska, A., Enters, D., Tylmann, W., 2016. Sedimentary
569 Bacteriopheophytin a as an indicator of meromixis in varved lake sediments of Lake Jaczno,
570 north-east Poland, CE 1891–2010. Glob. Planet. Change 144, 109–118.
571 https://doi.org/10.1016/j.gloplacha.2016.07.012

572 Cyr, H., McCabe, S.K., Nürnberg, G.K., 2009. Phosphorus sorption experiments and the
573 potential for internal phosphorus loading in littoral areas of a stratified lake. Water Res. 43,
574 1654–1666. https://doi.org/10.1016/j.watres.2008.12.050

575 Davidson, T.A. and Jeppesen, E., 2013. The role of palaeolimnology in assessing
576 eutrophication and its impact on lakes. J. Paleolimnol. 49, 391–410.
577 https://doi.org/10.1007/s10933-012-9651-0
578 Fiedor, J., Fiedor, L., Kammhuber, N., Scherz, A., Scheer, H., 2002. Photodynamics of the
579 Bacteriochlorophyll–Carotenoid System. 2. Influence of Central Metal, Solvent and β-
580 Carotene on Photobleaching of Bacteriochlorophyll Derivatives. Photochem. Photobiol. 76,
581 145–152. https://doi.org/10.1562/0031-8655(2002)076<0145:POTBCS>2.0.CO;2

582 Fischer, A., 1996. Isotopengeochemische Untersuchungen ($\delta^{18}O$ und $\delta^{13}C$) im Wasser und in
583 den Sedimenten des Soppensees (Kt. Luzern, Schweiz). Ph.D. Thesis, ETH, Zürich, pp.184.

584 Gao, L., Zhou, J.M., Yang, H., Chen, J., 2005. Phosphorus fractions in sediment profiles and
585 their potential contributions to eutrophication in Dianchi Lake. Environ. Geol. 48, 835–844.
586 https://doi.org/10.1007/s00254-005-0005-3

587 Gierga, M., Hajdas, I., van Raden, U.J., Gilli, A., Wacker, L., Sturm, M., Bernasconi, S.M.,
588 Smittenberg, R.H., 2016. Long-stored soil carbon released by prehistoric land use: evidence
589 from compound-specific radiocarbon analysis on Soppensee lake sediments. Quat. Sci. Rev.
590 144, 123–131. https://doi.org/10.1016/j.quascirev.2016.05.011

591 Gruber, N., Wehrli, B., Wüest, A., 2000. The role of biogeochemical cycling for the formation
592 and preservation of varved sediments in Soppensee (Switzerland). J. Paleolimnol. 24, 277–
593 291. https://doi.org/10.1023/A:1008195604287

594 Hajdas, I., Michczyński, A., 2010. Age-depth model of Lake Soppensee (Switzerland) based
595 on the high-resolution ^{14}C chronology compared with varve chronology. Radiocarbon 52,
596 1027–1040. https://doi.org/10.1017/S0033822200046117

597 Hao, J., Knoll, A.H., Huang, F., Schieber, J., Hazen, R.M., Daniel, I., 2020. Cycling phosphorus
598 on the Archean Earth: Part II. Phosphorus limitation on primary production in Archean
599 ecosystems. Geochim. Cosmochim. Acta 280, 360–377.
600 https://doi.org/10.1016/j.gca.2020.04.005

Heiri, O., Ilyashuk, B., Millet, L., Samartin, S., Lotter, A.F., 2015. Stacking of discontinuous regional palaeoclimate records: chironomid-based summer temperatures from the Alpine region. Holocene 25, 137–149. https://doi.org/10.1177/0959683614556382

Hofmann, W., 2001. Late-Glacial/Holocene succession of the chironomid and cladoceran fauna of the Soppensee (Central Switzerland). J. Paleolimnol. 25, 411–420. https://doi.org/10.1023/A:1011103820283

Jeffrey, S.t., Humphrey, G., 1975. New spectrophotometric equations for determining chlorophylls a, b, c1 and c2 in higher plants, algae and natural phytoplankton. Biochem. Physiol. Pflanz. 167, 191-–194. https://doi.org/10.1016/S0015-3796(17)30778-3

Kapanen, G., 2008. Phosphorus fractionation in lake sediments. Estonian J. Ecol. 57, 244–255. doi: 10.3176/eco.2008.4.02

Katsev, S., Dittrich, M., 2013. Modeling of decadal scale phosphorus retention in lake sediment under varying redox conditions. Ecol. Model. 251, 246–259. https://doi.org/10.1016/j.ecolmodel.2012.12.008

Kind, J., Raden, U.J.v., García-Rubio, I., Gehring, A.U., 2012. Rock magnetic techniques complemented by ferromagnetic resonance spectroscopy to analyse a sediment record. Geophys. J. Int. 191, 51–63. https://doi.org/10.1111/j.1365-246X.2012.05620.x

Kirilova, E., Heiri, O., Enters, D., Cremer, H., Lotter, A.F., Zolitschka, B., Huebener, T., 2009. Climate-induced changes in the trophic status of a Central European lake. J. Limnol. 68, 71–82. https://doi.org/10.4081/jlimnol.2009.71

Langenegger, T., Vachon, D., Donis, D., McGinnis, D.F., 2019. What the bubble knows: Lake methane dynamics revealed by sediment gas bubble composition. Limnol. Oceanogr. 64, 1526–1544. https://doi.org/10.1002/lno.11133

624 Lepori, F., Roberts, J.J., 2017. Effects of internal phosphorus loadings and food-web structure
625 on the recovery of a deep lake from eutrophication. J. Great Lakes Res. 43, 255–264.
626 https://doi.org/10.1016/j.jglr.2017.01.008

627 Lotter, A.F., 1989. Evidence of annual layering in Holocene sediments of Soppensee,
628 Switzerland. Aquat. Sci. 51, 19–30. https://doi.org/10.1007/BF00877778

629 Lotter, A.F., 1999. Late-glacial and Holocene vegetation history and dynamics as shown by
630 pollen and plant macrofossil analyses in annually laminated sediments from Soppensee,
631 central Switzerland. Veg. Hist. Archaeobot. 8, 165–184. https://doi.org/10.1007/BF02342718

632 Lotter, A.F., 2001. The palaeolimnology of Soppensee (Central Switzerlabnd), as evidenced
633 by diatom, pollen, and fossil-pigment analyses. J. Limnol. 25, 65–79.
634 https://doi.org/10.1023/A:1008140122230

635 Makri, S., Rey, F., Gobet, E., Gilli, A., Tinner, W., Grosjean, M., 2020. Early human impact in
636 a 15,000-year high-resolution hyperspectral imaging record of paleoproduction and anoxia
637 from a varved lake in Switzerland. Quat. Sci. Rev. 239, 106335.
638 https://doi.org/10.1016/j.quascirev.2020.106335

639 Makri, S., Lami, A., Tu, L., Tylmann, W., Vogel, H., Grosjean, M., 2021. Holocene phototrophic
640 community and anoxia dynamics in meromictic Lake Jaczno (NE Poland) using high-
641 resolution hyperspectral imaging and HPLC data. Biogeosciences 18, 839–1856.
642 https://doi.org/10.5194/bg-2020-362

643 Müller, B., Lotter, A.F., Sturm, M., Ammann, A., 1998. Influence of catchment quality and
644 altitude on the water and sediment composition of 68 small lakes in Central Europe. Aquat.
645 Sci. 60, 316–337. https://doi.org/10.1007/s000270050044

646 Nürnberg, G.K., Fischer, R., Paterson, A.M., 2018. Reduced phosphorus retention by anoxic
647 bottom sediments after the remediation of an industrial acidified lake area: Indications from P,

Al, and Fe sediment fractions. Sci. Total Environ. 626, 412–422. https://doi.org/10.1016/j.scitotenv.2018.01.103

Ohno, T., Zibilske, L.M., 1991. Determination of low concentrations of phosphorus in soil extracts using malachite green. Soil Sci. Soc. Am. J. 55, 892–895. https://doi.org/10.2136/sssaj1991.03615995005500030046x

Orihel, D.M., Baulch, H.M., Casson, N.J., North, R.L., Parsons, C.T., Seckar, D.C., Venkiteswaran, J.J., 2017. Internal phosphorus loading in Canadian fresh waters: a critical review and data analysis. Can. J. Fish. Aquat. Sci. 74, 2005–2029. https://doi.org/10.1139/cjfas-2016-0500

R Core Team, 2017. R: A Language and Environment for Statistical Computing. Vienna, Austria.

Paasche, Ø., Larsen, J., 2010. Changes in lake stratification and oxygen distribution inferred from two contrasting records of magnetotactic bacteria and diatoms. J. Geophys. Res. Biogeosci. 115, G02012. https://doi.org/10.1029/2009JG001081

Paasche, Ø., Løvlie, R., Dahl, S.O., Bakke, J., Nesje, A., 2004. Bacterial magnetite in lake sediments: late glacial to Holocene climate and sedimentary changes in northern Norway. Earth Planet. Sci. Lett. 223, 319–333. https://doi.org/10.1016/j.epsl.2004.05.001

Paerl, H.W., 1988. Nuisance phytoplankton blooms in coastal, estuarine, and inland waters. Limnol. Oceanogr. 33, 823–843. https://doi.org/10.4319/lo.1988.33.4part2.0823

Rey, F., Gobet, E., Schwörer, C., Hafner, A., Szidat, S.,Tinner, W., 2020. Climate impacts on vegetation and fire dynamics since the last deglaciation at Moossee (Switzerland). Clim. Past 16, 1347–1367. https://doi.org/10.5194/cp-16-1347-2020

Rivas-Lamelo, S., Benzerara, K., Lefèvre, C.T., Monteil, C.L., Jézéquel, D., Menguy, N., Viollier, E., Guyot, F., Férard, C., Poinsot, M., Skouri-Panet, F., Trcera, N., Miot, J., Duprat,

E., 2017. Magnetotactic bacteria as a new model for P sequestration in the ferruginous Lake Pavin. Geochem. Perspect. Lett. 5, 35–41. doi: 10.7185/geochemlet.1743

Royston, J.P., 1995. Shapiro-Wilk normality test and P-value. Appl. Stat., 44 547–551. https://doi.org/10.2307/2986146

Ruban, V., Brigault, S., Demare, D., Philippe, A.-M., 1999. An investigation of the origin and mobility of phosphorus in freshwater sediments from Bort-Les-Orgues Reservoir, France. J. Environ. Monit. 1, 403–407. https://doi.org/10.1039/A902269D

Ruban, V., Lopez-Sanchez, J.F., Pardo, P., Rauret, G., Muntau, H., Quevauviller, P., 2001. Development of a harmonised phosphorus extraction procedure J. Environ. Monit. 3, 121–125. https://doi.org/10.1039/B005672N

Rydin, E., 2000. Potentially mobile phosphorus in Lake Erken sediment. Water Res. 34, 2037–2042. https://doi.org/10.1016/S0043-1354(99)00375-9

Schaller, T. and Wehrli, B., 1996. Geochemical-focusing of manganese in lake sediments—an indicator of deep-water oxygen conditions. Aquat. Geochem. 2, 359–378. https://doi.org/10.1007/BF00115977

Schneider, T., Rimer, D., Butz, C., Grosjean, M., 2018. A high-resolution pigment and productivity record from the varved Ponte Tresa basin (Lake Lugano, Switzerland) since 1919: insight from an approach that combines hyperspectral imaging and high-performance liquid chromatography. J. Paleolimnol. 60, 381–398. https://doi.org/10.1007/s10933-018-0028-x

Schnurrenberger, D., Russell, J., Kelts, K., 2003. Core description Classification of lacustrine sediments based on sedimentary components. J. Paleolimnol. 29, 141–154. https://doi.org/10.1023/A:1023270324800

Søndergaard, M., Jensen, P.J., Jeppesen, E., 2001. Retention and internal loading of phosphorus in shallow, eutrophic lakes. Sci. World J. 1, 427–442. https://doi.org/10.1100/tsw.2001.72

697 Steinsberger, T., Schmid, M., Wüest, A., Schwefel, R., Wehrli, B., Müller, B., 2017. Organic
698 carbon mass accumulation rate regulates the flux of reduced substances from the sediments
699 of deep lakes. Biogeosciences 14, 3275–3285. https://doi.org/10.5194/bg-14-3275-2017

700 Straile, D., Jöhnk, K., Henno, R., 2003. Complex effects of winter warming on the
701 physicochemical characteristics of a deep lake. Limnol. Oceanogr. 48, 1432-1438.
702 https://doi.org/10.4319/lo.2003.48.4.1432

703 Tu, L., Jarosch, K.A., Schneider, T., Grosjean, M., 2019. Phosphorus fractions in sediments
704 and their relevance for historical lake eutrophication in the Ponte Tresa basin (Lake Lugano,
705 Switzerland) since 1959. Sci. Total Environ. 685, 806–817.
706 https://doi.org/10.1016/j.scitotenv.2019.06.243

707 Tu, L., Zander, P., Szidat, S., Lloren, R., Grosjean, M., 2020. The influences of historic lake
708 trophy and mixing regime changes on long-term phosphorus fraction retention in sediments of
709 deep eutrophic lakes: a case study from Lake Burgäschi, Switzerland. Biogeosciences 17,
710 2715–2729. https://doi.org/10.5194/bg-17-2715-2020

711 van Raden, U.J., 2012. High-resolution swiss lake records of climate change. Ph.D. Thesis,
712 ETH, Zürich, Nr 20596, https://doi.org/10.3929/ethz-a-009783578.

713 Vuillemin, A., Friese, A., Wirth, R.A., Schuessler, J.M., Schleicher, A., Kemnitz, H., Lücke,
714 A.W., Bauer, K., Nomosatryo, S., Von Blanckenburg, F., Simister, R.G., Ordoñez, L., Ariztegui,
715 D., Henny, C.M., Russell, J., Bijaksana, S., Vogel, H.A., Crowe, S., Kallmeyer, J., 2020.
716 Vivianite formation in ferruginous sediments from Lake Towuti, Indonesia. Biogeosciences 17,
717 1955–1973. https://doi.org/10.5194/bg-17-1955-2020

718 Wei, T., Simko, V., 2017. R Package “Corrplot”: Visualization of a Correlation Matrix. Wickham,
719 H., 2016. ggplot2: Elegant Graphics for Data Analysis.

720 Williams, J., Jaquet, J., Thomas, R., 1976. Forms of phosphorus in the surficial sediments of
721 Lake Erie. Can. J. Fish. Aquat. 33, 413–429. https://doi.org/10.1139/f76-063

Worsfold, P., McKelvie, I., Monbet, P., 2016. Determination of phosphorus in natural waters: A historical review. Anal. Chim. Acta 918, 8–20. https://doi.org/10.1016/j.aca.2016.02.047

Zander, P.D., Żarczyński, M., Vogel, H., Tylmann, W., Wacnik, A., Sanchini, A., Grosjean, M., 2021. A high-resolution record of Holocene primary productivity and water-column mixing from the varved sediments of Lake Żabińskie, Poland. Sci. Total Environ. 755, 143713. https://doi.org/10.1016/j.scitotenv.2020.143713

Zarczynski, M., Wacnik, A., Tylmann, W., 2019. Tracing lake mixing and oxygenation regime using the Fe/Mn ratio in varved sediments: 2000year-long record of human-induced changes from Lake Zabinskie (NE Poland). Sci. Total Environ. 657, 585–596. https://doi.org/10.1016/j.scitotenv.2018.12.078

Zhu, M., Zhu, G., Li, W., Zhang, Y., Zhao, L., Gu, Z., 2013. Estimation of the algal-available phosphorus pool in sediments of a large, shallow eutrophic lake (Taihu, China) using profiled SMT fractional analysis. Environ. Pollut. 173, 216–223. https://doi.org/10.1016/j.envpol.2012.10.016

Captions:

Fig. 1. (a) Map of Switzerland with the location of Soppensee. (b) Aerial image of the catchment area of Soppensee (inside the blue polygon; background map © swisstopo) and a bathymetric map of the lake with the coring site. (c) Age–depth model and lithology of Core So08-3 and, on the left, the six lithological units A-F according to Gierga et al. (2016). LST marks the Laacher See Tephra at 521–521.5 cm depth.

Fig. 2. Time series of HSI-inferred pigment data, five P fractions concentrations (µg g^{-1} dry weight; DW and selected XRF data (Fe, Mn and Ca). For the pigment data, purple and green lines show the data at highest resolution (~75 µm) and red lines are 2-cm aggregate averages (267 samples). The vertical dashed lines represent the lower and upper limits of the calibration models (refer to Fig. S3 in the supplementary material). The Bphe-*a* and green pigments serve as proxies of lake paleoproduction and anoxia/meromixis, respectively. The appearance of Fe- and Mn-rich laminae (with siderite) and biogenic calcite varves in sediments was taken from Fischer (1996). MTB: Magnetotactic bacteria, detected by Kind et al. (2012). The horizontal dashed grey lines separate the different units (A to F; Gierga et al. 2016). Note the different scales of the x-axes. (For interpretation of the references to color in this figure legend, the reader is referred to the web version of this article.)

Fig. 3. Example sections from four phases showing 2-cm sediment core sections (sediment depth of the composite core) covering approximately 40 years according to the age-depth model in Fig. 1c; variations of Bphe-*a* (in purple) and green pigments (in green) are shown with the spectral indices and the calibrated pigment concentrations at high resolution (~75 µm). For each image, the vertical red lines show the 2-mm-wide window used for determining the spectral-index time series for the individual core section; the three grey lines represent the mean value and standard deviations of the two spectral indices for the entire sediment core; and the vertical yellow lines represent the lower limits of the calibration models. a) close-up section from the Allerød interstadial: this is a period with high lake primary production and high Bphe-*a* concentrations, indicating anoxia. b) close-up section from the Younger Dryas (YD), showing decreased lake primary production and almost absent Bphe-*a*,

concurrent with Fe- and Mn-rich layers (Fischer, 1996), suggesting a seasonally mixed hypolimnion. c) close-up section from the mid-Holocene: showing high primary production and persistently high Bphe-*a* concentrations, which suggests strongly stratified conditions with anoxia or even meromixis. d) close–up section from the late Holocene, showing high lake production and low Bphe-*a* concentrations in Fe- and Mn-rich sediments, which suggests mostly a well oxygenated water column. The calibration model is valid for green pigments between 13.6 and 321.8 µg g^{-1} dry sediments and for Bphe-*a* between 9.7 and 233.3 µg g^{-1} dry sediments (Fig. S3). (For interpretation of the references to color in this figure legend, the reader is referred to the web version of this article.)

Fig. 4. Comparison of millennial- and centennial-scale variations of Soppensee trophic status with sediment Fe-P (labile P) data over the Late-glacial and Holocene. (a) Chironomid July temperatures from the Alpine region (Heiri et al., 2015). (b) Percentage of arboreal pollen (AP) including tree and shrub pollen (Lotter, 2001). (c) The diatom-inferred past epilimnetic total phosphorus (DI-TP) concentrations in Soppensee (Lotter, 2001); the dashed black line represents the mean value of the DI-TP record (30 µg L^{-1}). (d) Record of Fe-P concentrations in sediments (µg g^{-1} dry weight, DW); the dashed black line represents the mean value of the Fe-P record at 2267 µg/g DW. (e) The anoxia and (f) aquatic paleoproduction proxies are shown as 100-year running means. The yellow and green vertical bars at the top of the figure highlight the Late-glacial Allerød interstadial and the Younger Dryas (YD) cold period, respectively (according to Gierga et al. 2016). Phase a to Phase d refer to Fig. 5. In (c)-(e), dashed red (blue) lines mark relative maxima (minima) in lake paleoproduction/anoxia synchronously with relative minima (maxima) of Fe-P in sediments. (For interpretation of the references to color in this figure legend, the reader is referred to the web version of this article.)

Fig. 5. Conceptual model of four phases (a to d) of lake primary production, mixing regime, P cycling in a small deep eutrophic lake (like Soppensee) during the Holocene (Section 5.2). MTB: magnetotactic bacteria; PSB: purple sulfur bacteria; OM: organic matter. Note that, overall, the illustrated sizes of Fe-P among different phases indicate the relative amounts of Fe-P in sediments; the bottom-water (brown-green color) in (c)-(d) represents anoxia during seasonal stratifications. Parts of the symbols for this figure were taken from Symbols courtesy of the Integration and Application Network

(ian.umces.edu/symbols/). (For interpretation of the references to color in this figure legend, the reader is referred to the web version of this article.)

Figure 1

Click here to access/download;Figure;Figure 1_R1.eps

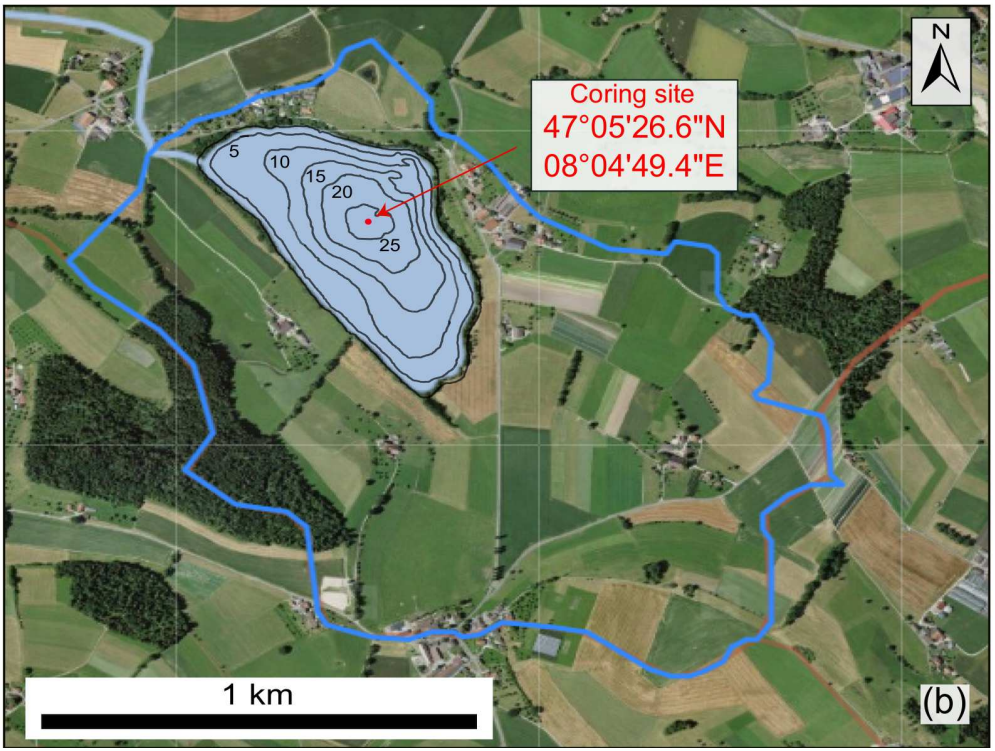

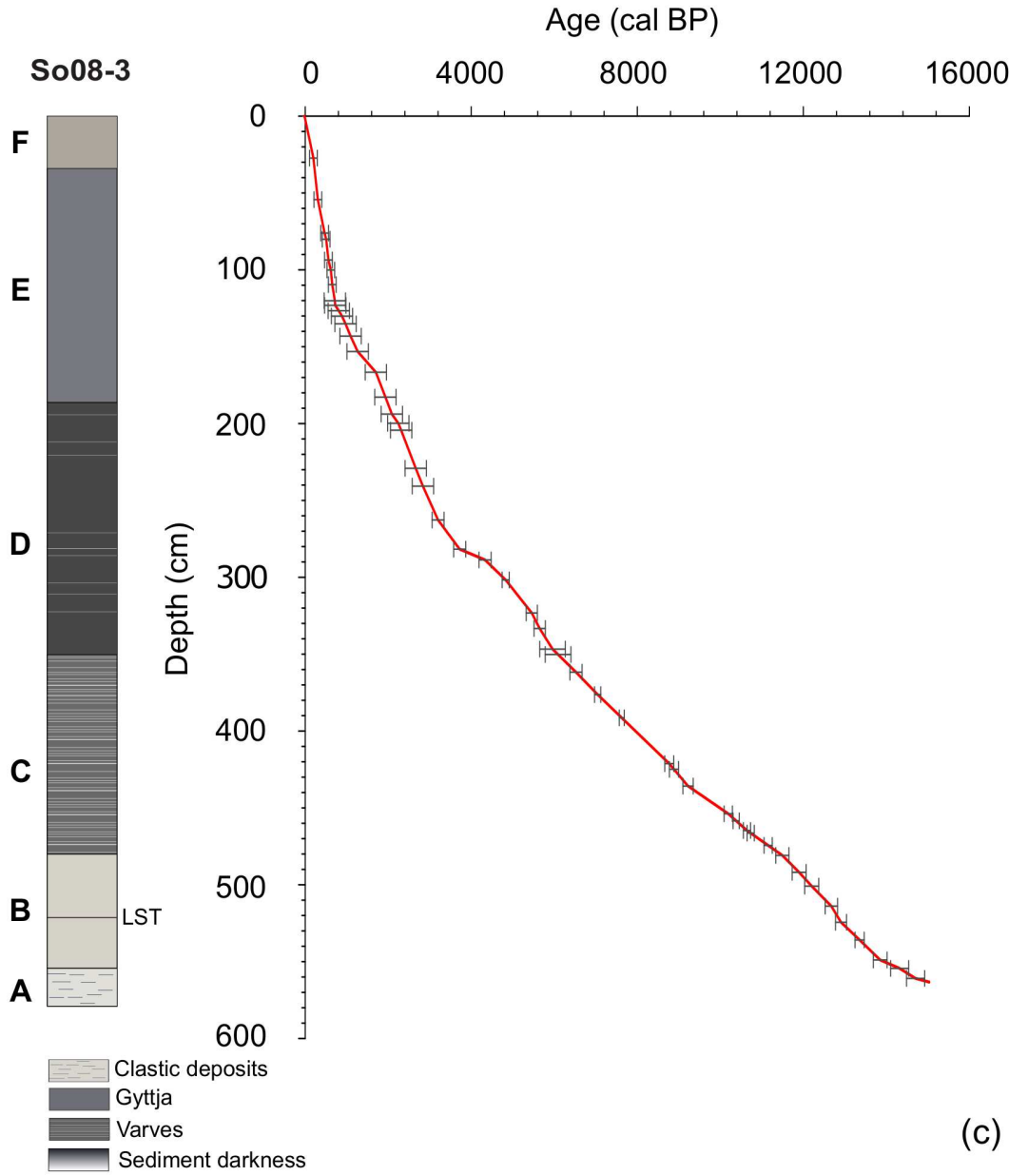

Figure 2

Click here to access/download;Figure;Figure 2_R1.eps

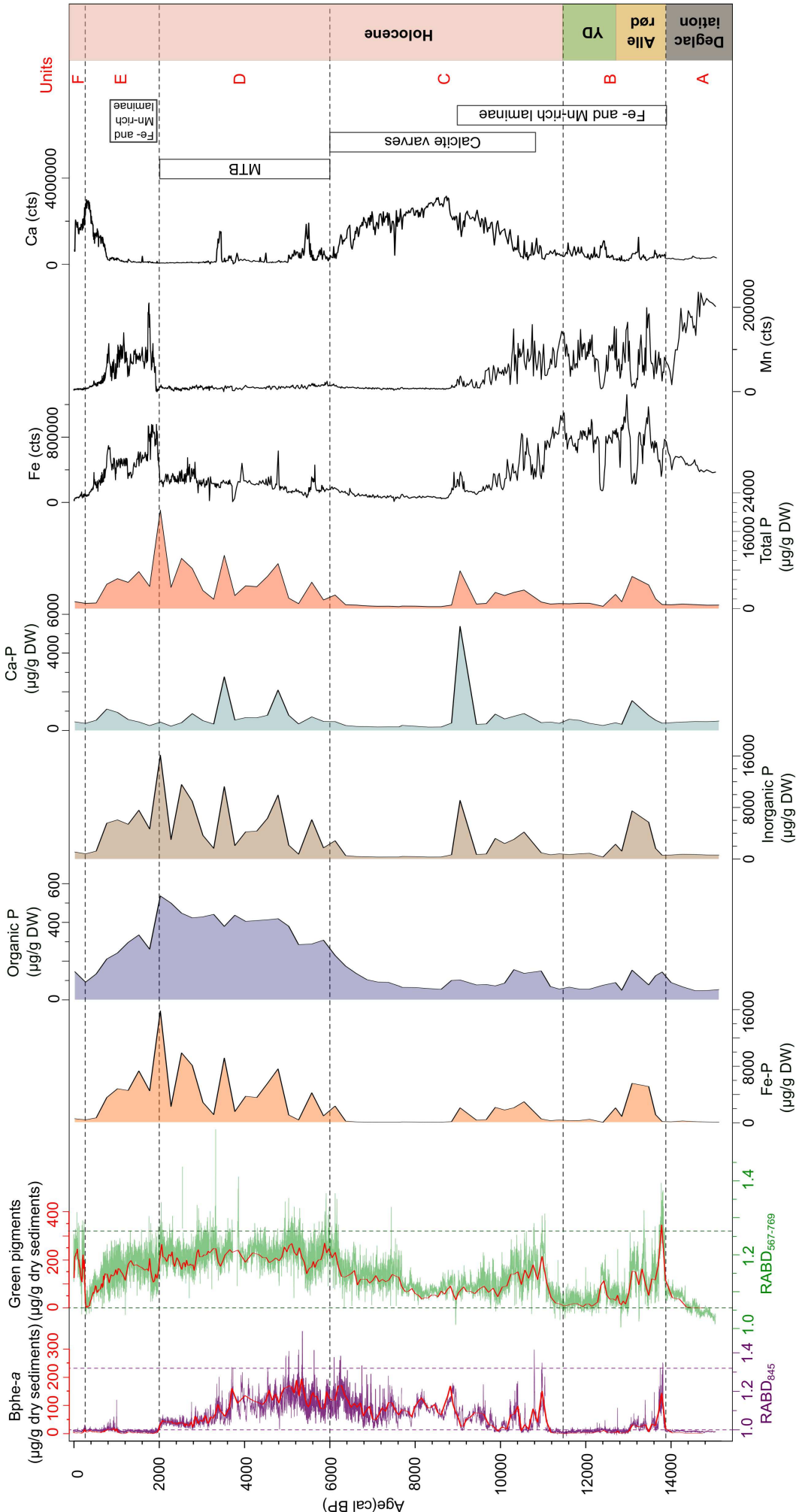

Figure 3

Click here to access/download;Figure;Figure 3_R1.eps

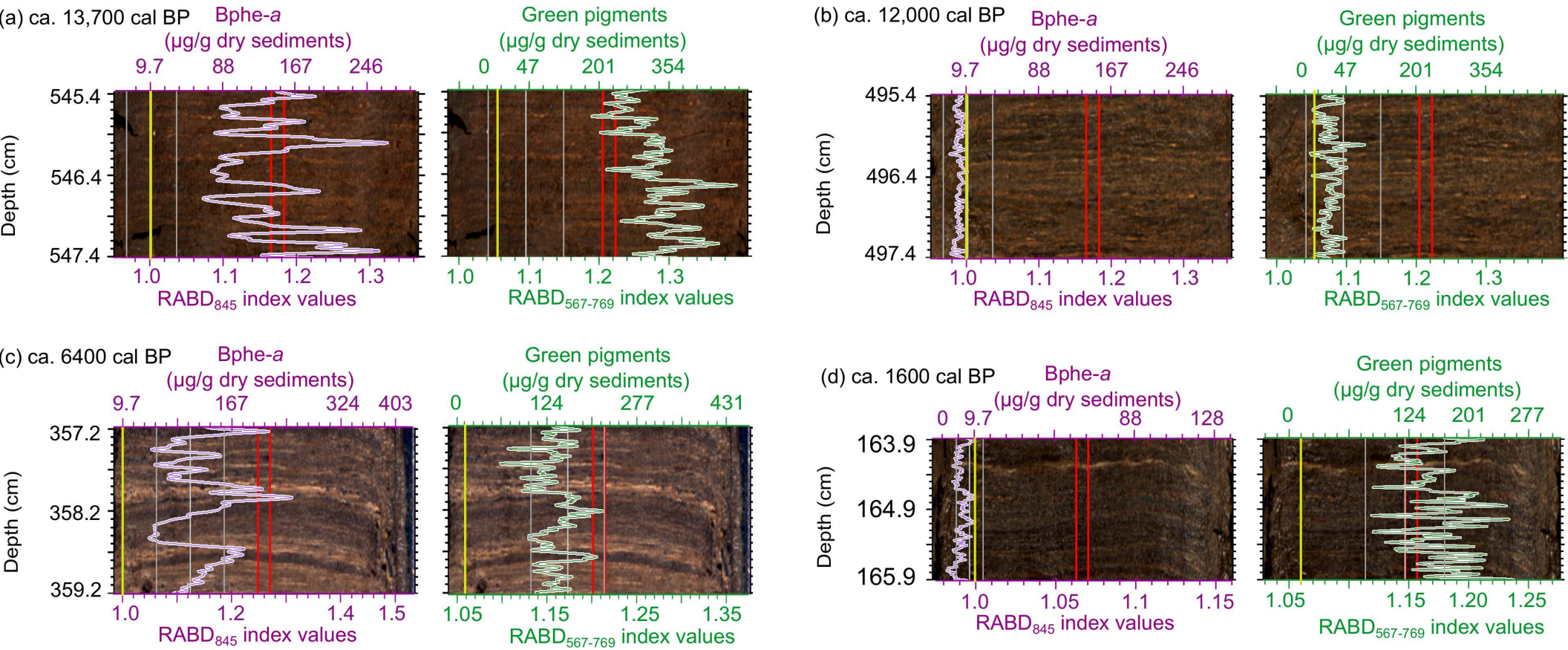

Figure 4

Click here to access/download;Figure;Figure 4_R1.eps

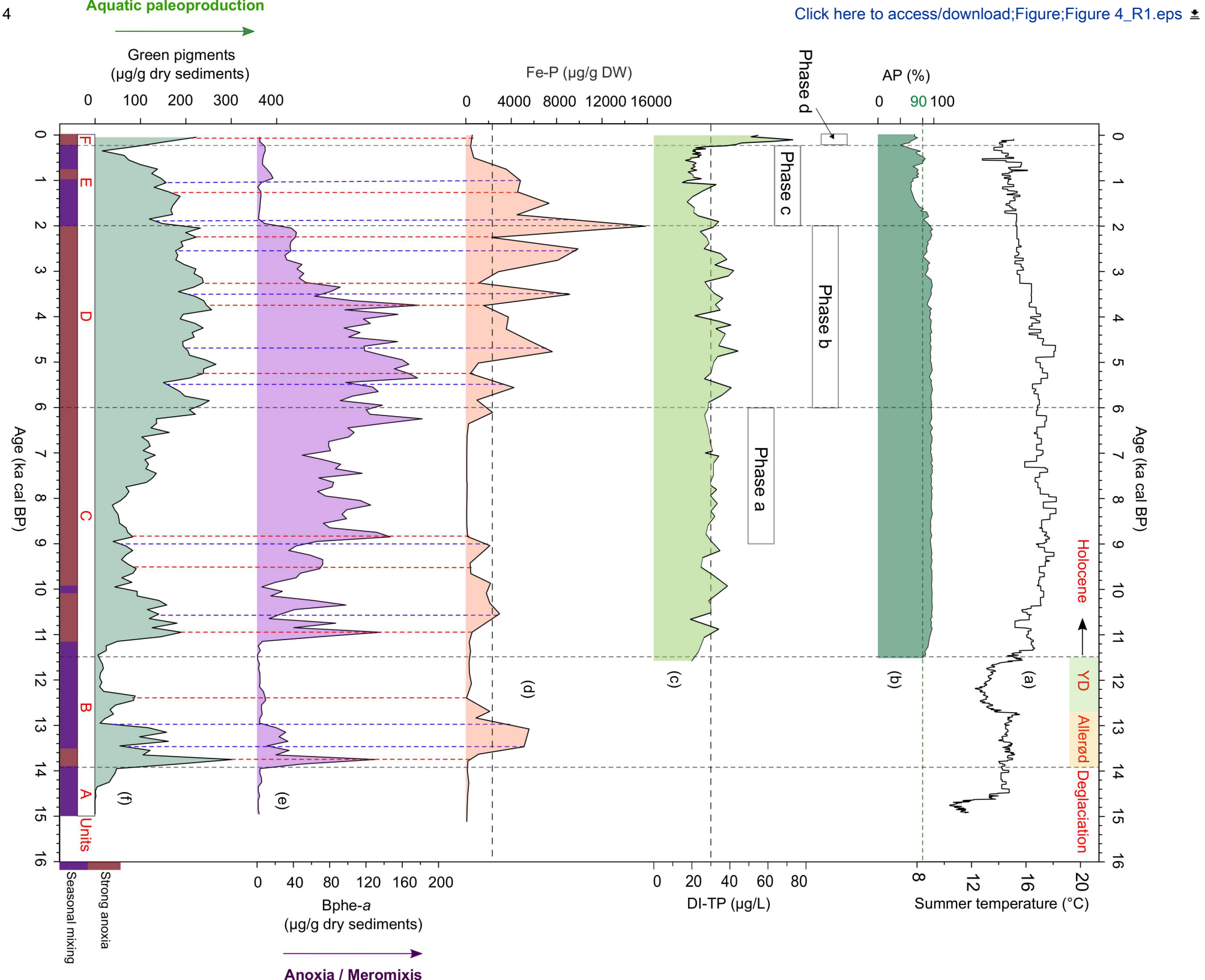

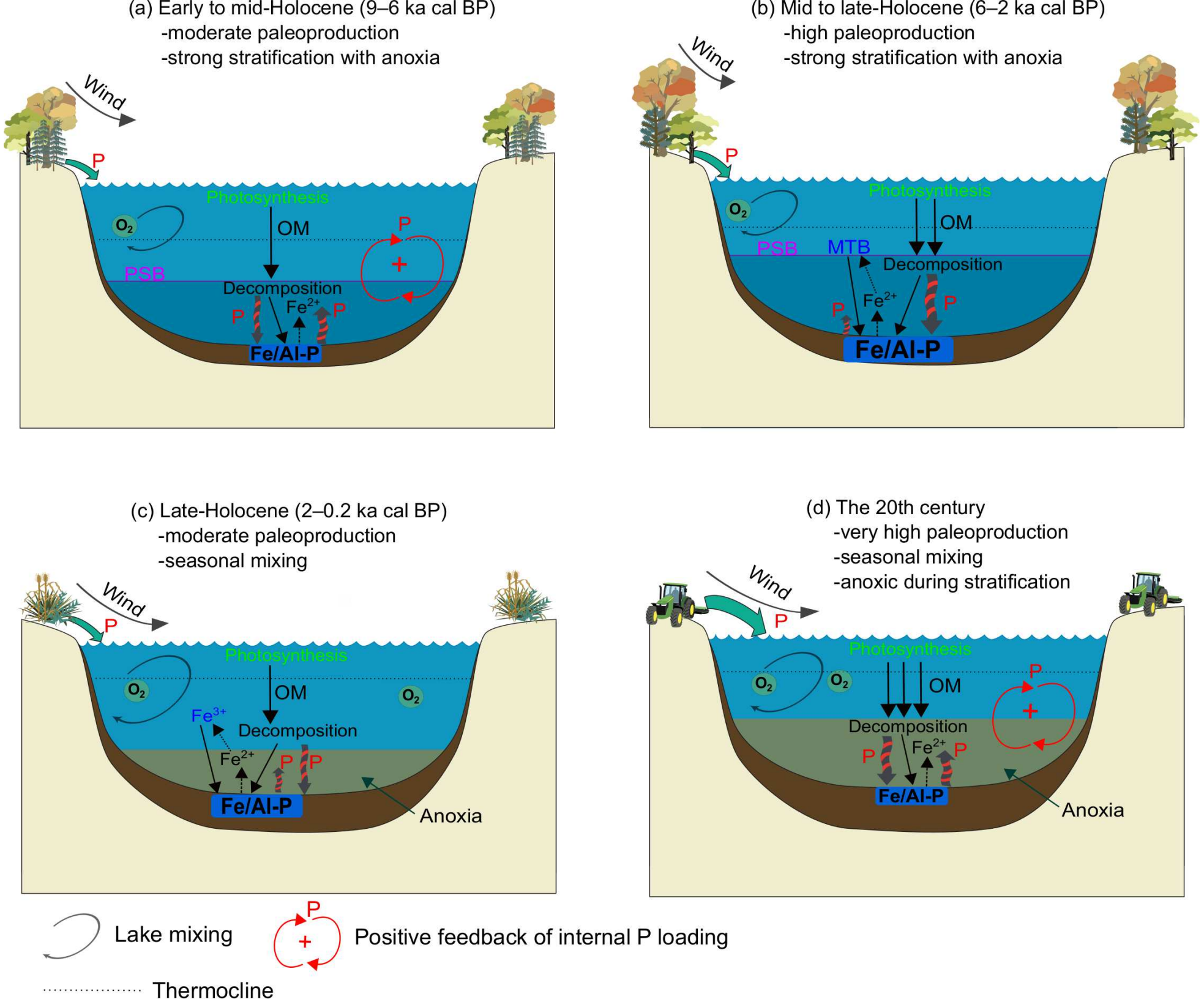

Figure 5

Click here to access/download;Figure;Fig. 5_R1.eps

Declaration of interests

☒ The authors declare that they have no known competing financial interests or personal relationships that could have appeared to influence the work reported in this paper.

☐The authors declare the following financial interests/personal relationships which may be considered as potential competing interests: